The Enhanced Morlet Transform via Iterative Filter to Study Turbulent Data Strings

Y.-N.Jeng [1] , C.-T. Chen[2] and Y.-C. Cheng [3]

1. Department of Aeronautics and Astronautic, National Cheng-Kung University, Tainan, Taiwan
z6208016@email.ncku.edu.tw
2. Department of Aeronautics and Astronautics, National Cheng Kung University, Tainan, Taiwan
3. Department of Electrical Engnieering, National Taiwan University, Taipei, Taiwan

Corresponding author ***Y.-N. Jeng***

Abstract

The function of the continuous wavelet (Morlet) transform is enhanced by adding a windowed spectrum via the iterative filter corresponding to the scale function. The Jeng, Huang and Chen iterative filter is properly employed so that the windowing procedure on the spectrum domain can be accurately done. The bandwidth of the resulting two-dimensional wavelet coefficient plot of a single sine function is narrower than that generated by the original Morlet transform. Subsequently, the visibility of the wavelet coefficient plot of several waves with frequencies closing to each other is significantly improved. The application of the proposed wavelet transform to the velocity data string of a low speed turbulent wake flow after a blunt body clearly shows many details which are not known before. On the resulting wavelet coefficient plots, many frequency splitting and merging procedures between waves can be easily captured. It seems that the present method might be considered as a well organized validation tool to compare the direct numerical simulation and corresponding experimental data.

Key words: *Enhanced Morlet Transform, Windowed Spectrum, Turbulent Data String.*

1. Introduction

The study upon a turbulent flow field is seriously restricted by the fact that there is not effective tool to look into the details. In spite of the fact that many turbulent data can be easily and effectively collected, people can only calculate the overall Fourier spectrum, turbulent kinetic energy, and a few other lumped properties. Together with results of the Direction Numerical Simulation (DNS) and flow visualization, people do grasp many physical insights. However, precise interpretation of the effect of numerical error upon a DNS data is still an open and difficult issue. The development of flow visualization is still far away from the stage of clearly providing detailed information of a turbulent flow field. As a consequence, people can only understand a turbulent flow field to a limited extend.

As the continuous wavelet transform was introduced to study turbulent flow [1-4], many studies followed up [5-13] because they agreed with the view point of Farge that the Morlet transform can provide the local information of spectrum. Unfortunately, there are not much detailed information can be directly obtained from the resulting wavelet coefficient plot. Therefore, people have to employ other techniques to extract desired information from the resulting wavelet coefficient plot. In fact, a continuous wavelet transform is a generalized short time Fourier series expansion whose visibility is deteriorated by the present of non-periodic and non-sinusoidal parts. Recently, the present authors [14] used a simple fast Fourier transform with small low frequency error to find the spectrum of the data string provided that the non-sinusoidal and low frequency parts are excluded by the iterative filter of Ref.[15]. Then, the spectrum is employed to give a band-passed data string before the Morlet transform is calculated. The resulting two-dimensional wavelet coefficient plot has a much better visibility than that of the original Morlet transform. However, the spectrum is evaluated in terms of the high frequency part of the whole data string such that the local property is deteriorated. Consequently, if the bandwidth of the band-passed filter become more and more thin, the resulting two-dimensional wavelet coefficient shrinks to be the Fourier spectrum which does not reflect any local behaviour. In this study, the band-passed data is given by employing the iterative filter of Ref.[15]. Subsequently, the iterative filter will also be employed to prevent the Morlet transform from collecting too many information. Moreover, the local behaviour of the iterative filter will prevent the drawback of the enhanced Morlet transform proposed in Ref.[14].

2. Theoretical Analysis

Assume that a discrete data string can be approximated by

$$y(t) = \sum_{n=0}^{N} b_n \cos\left(\frac{2\pi t}{\lambda_n}\right) + c_n \sin\left(\frac{2\pi t}{\lambda_n}\right) \qquad (1)$$

In Ref.[14], it was proven that after applying the Gaussian smoothing once, the resulting smoothed data becomes

$$\bar{y}_1(t) \approx \sum_{n=0}^{N} a(\sigma/\lambda_n)\{b_n \cos\left(\frac{2\pi t}{\lambda_n}\right) + c_n \sin\left(\frac{2\pi t}{\lambda_n}\right)\} \qquad (2)$$

where $a(\sigma/\lambda_n)$ is the attenuation factor introduced by the smoothing and can be proven numerically that

$$0 \le a(\sigma/\lambda_n) \approx \exp[-2\pi^2\sigma^2/\lambda_n^2] \le 1 \qquad (3)$$

If the removed high frequency part is denoted as y_1' and apply the same smoothing to it to obtain the second smoothed result as $\bar{y}_2$ and repeat the same procedure to obtain the $m-$th smoothed and high frequency part as $\bar{y}_m$ and y_m', respectively. The following relation can be built

$$y'_m = \sum_{n=0}^{N}[1-a(\sigma/\lambda_n)]^m\left[b_n\cos\left(\frac{2\pi t}{\lambda_n}\right)+c_n\sin\left(\frac{2\pi t}{\lambda_n}\right)\right]$$

$$\bar{y}(m) = \bar{y}_1 + \bar{y}_2 + ... + \bar{y}_m =$$

$$= \sum_{n=0}^{N}\{1-[1-a(\sigma/\lambda_n)]^m\}\left[b_n\cos\left(\frac{2\pi t}{\lambda_n}\right)+c_n\sin\left(\frac{2\pi t}{\lambda_n}\right)\right] \qquad (4)$$

$\bar{y}(m)$ can be considered as the smoothed part and y'_m as the high frequency part. It was proven in Ref.[15] that the transition region from $\{1-[1-a(\sigma/\lambda_n)]^m\}$ = 0 to 1 is much narrower than that of the original $a(\sigma/\lambda_n)$. It should be noted that, like the property given by the original Gaussian smoothing method, the smoothed part $\bar{y}(m)$ preserves the local behaviour of the original data to certain extend.

The following Morlet transform transfer a data string $y(t)$ into the wavelet coefficient.

$$W(a,\tau) = \frac{1}{\sqrt{a}}\int_{-\infty}^{\infty} y(x)\psi^*(\frac{x-\tau}{a})dx \qquad (5)$$

where $\psi(x) = e^{i6x}e^{-|x|^2/2}$ and a is called as the scale function. If this transform is applied over a range $a_0 \le a \le a_1$, a two-dimensional wavelet coefficient plot is obtained on the (a,τ) plane. By applying Eq.(5) to Eq.(1), it can be easily shown that

$$W(a,\tau) \approx \sum_{n=0}^{N} b_n\sqrt{\frac{\pi a}{2}}\exp\left(-\frac{a^2}{2}\left(\frac{2\pi}{\lambda_n}-\frac{6}{a}\right)^2\right)\left[\cos\frac{2\pi\tau}{\lambda_n}+i\sin\frac{2\pi\tau}{\lambda_n}\right]$$

$$+\sum_{n=0}^{N} c_n\sqrt{\frac{\pi a}{2}}\exp\left(-\frac{a^2}{2}\left(\frac{2\pi}{\lambda_n}-\frac{6}{a}\right)^2\right)\left[\sin\frac{2\pi\tau}{\lambda_n}-i\cos\frac{2\pi\tau}{\lambda_n}\right] \qquad (6)$$

A careful inspection upon this formula reveals that the original Morlet transform collects too much information into a single line with a = constant. For example, consider a test function of $y = \sin(8\pi t)$, $0 \le t \le 20$ the response of $W(a,\tau)$ at $\tau = 9.0625$ is shown as the dotted line in Fig.1. It seems that, at all the positions of a in the range of $0.4\lambda \le a \le 1.7$ (say, $0.7 < \lambda/a < 2.5$ in the figure), $W(a,\tau)$ gives a non-zero response. In an ideal situation, it would be better to obtain a delta form response. However, as noted in Ref.[16,17], there is an uncertainty range, say

$$\sigma_t^2\sigma_\omega^2 \ge 1/4$$

$$\sigma_\tau = \int_{-\infty}^{\infty}(t-\tau)^2\exp[-((t-\tau)^4/4\sigma^4]dt$$

$$\sigma_\omega = \int_{-\infty}^{\infty}(p-\omega)^2\exp[-((p-\omega)^4/4\sigma_\omega{}^4]dt \qquad (7)$$

where σ_t^2 and σ_ω^2 are the uncertain variances in time and frequency domain, and $\omega = 2\pi f = 2\pi / \lambda$. In other words, if one shrink the information in the $a-$direction into a delta function, the uncertainty in time direction will be infinitely large. In order to obtain a good resolution in both time and frequency directions, a finite bandwidth in $a-$direction.

In order to shrink the range of collection information, before evaluating the wavelet coefficient at a given a value. The wavelength with a maximum response is considered as the central frequency. The iterative filter is then iterative searched to find a best fit. For example, Fig.1 is the result of applying the iterative filter with $\sigma / a = 0.535$ and 100 iteration steps. In the figure, the dashed line is the response of the iterative filter which is an one-sided filter only. The overall response shown as the solid line is the product between the original factor and that introduced by the filter. This filter parameter makes the maximum overall response of the original transform is not changed. Fig.2a is the result of using two-steps filter, with 100 iterations and $\sigma_L = 0.535$ to cut the long wave part and $\sigma_H = 0.95 * \sigma_L$ to cut the short wave part. It is seen that the overall response gives a non-zero response shorter than that of the original Morlet transform. Since the overall response is different from the maximum response of the Morlet transform, it is further scaled by a proper factor to obtain the a coincided overall response as shown in Fig.2b. Figure 3 shows the necessary data of (σ_L, m) to achieve the coincided maximum overall response with the original Morlet transform, where m is the necessary iteration cycles. For the sake of clarity, three different results of employing different σ's (and hence m's) to provide different windowing sizes are shown in Fig.4. A careful inspection upon Figs.3 and 4 reveals that a narrower window size should be equipped with a larger number of iteration of the filter and the increment is in an exponential form.

Results and Discussions

Now the experimental data of Ref.[10] is employed to demonstrate the present enhanced wavelet transform. The $u-$velocity data at $5d$ and $3d$ downstream location along the centerline of the blunt body's wake region is examined (see Fig.5a), respectively, where $d = 32\text{mm}$ is the width of the blunt body and Re_d =16500 is employed. The location of $5d$ is at the downstream point after the wake region (ended at about $2d$). The removed smoothed part corresponding to this data string is shown in Fig.5b. It is obviously that if this part is not removed, the corresponding spectrums will involve their contribution over the whole spectrum domain which introduces certain error. The resulting spectrum is shown in Fig.6. From this spectrum, it is obviously seen that dominate and three sub-harmonic modes can be easily captured. Note that, if the non-periodic part is not removed, the second and third the sub-

harmonic modes can not be easily captured. Generally, the third mode might be ignored because it is interfered by the low frequency error.

The wavelet coefficient plots generated by the original Morlet transform are shown in Fig.7 and that generated by the present improved transform are shown in Fig.8, respectively. In Fig.7, both the amplitude (often called as wavelet energy) and real part plots can not provide much information. On the other hand, the present method can give many information of how the dominate and sub-harmonic modes persist. Both the energy (amplitude) and real part of Fig.8 show that the vortex shedding information $x = 0.5d$ presents in a piecewise manner which can be seen along the line of $a = 0.0133$ (≈ 72 Hz and $\mathrm{St} = fd/U_0 = 0.305$). Many sub-harmonic modes also present in the same piecewise manner. Moreover, the frequency splitting and merging can be seen here and there between these dominate and sub-harmonic modes. It seems that from the real part plot one can get a more direct feeling upon the feature than that of the amplitude plot because the phase information give us a direction impression about the flow oscillation. The result shown in Fig.8 reflects that the vortex shedding does not give a perfect continuous spectrum line around the $a = 0.0133$ line. This is true because a vortex shedding from the inclined surface of the blunt body shown in Fig.3a can not always generate a regular and well structured vortex as can be seen from the flow visualization plot of Ref.[10]. Moreover, the high order sub-harmonic modes can not exactly persist their frequencies at exactly the integer multiples of the dominate frequency, say integer multiples of $a = 0.0133$. Part of the information of the energy cascade can be found by examining many left and right inclined waves between the dominate and the first sub-harmonic modes of Fig.8.

Since the experimental facilities does not involve a high speed camera and flow visualization via laser sheet splitting, the flow structure corresponding to all the details of frequency splitting and merging between waves of different wavelengths can not be exactly addressed. It seems that systematic restudies about this and many other turbulent flow fields are necessary so that the physics of the frequency splitting and merging can be correctly captured.

After one can clearly understand most physical meanings of the frequency splitting, the present method can also be employed as a code validation of a Direct Numerical Simulation (DNS) code. Today it is not easy to identify the role of numerical error in a DNS program. If both experimental data string measured at a point and the corresponding DNS result are available, the present method provide a tool to compare the features of them such that their error can be essentially identified.

Conclusions

A new tool to inspect a complicated data string of a turbulent flow field was successfully developed by enhancing the Morlet transform. The visibility of the resulting wavelet coefficient plot along the frequency direction is significantly recovered by employing an iterative filter to remove the low frequency error of the Fourier spectrum and exclude extra-information folded. Many resulting turbulent flow details on the spectrum domain are first seen so that they can only be partially explained. It seems that systematic and well organized experiments are necessary to obtain a fully understanding about a turbulent flow field. Besides, further developments upon many fields related to complicated data strings can be started by employing the present modifications upon the Fourier spectrum and continuous wavelet transform. A series of study upon brain, neural, and earth quake signals are on the way.

Acknowledgement

The authors acknowledge the support by the National Science Council, Republic of China, for this research under contract NSC-93-2212-E006-037. The experimental data was given by my colleague, Prof. Miau, and Dr. Wang and are gratefully acknowledged.

Reference

1. A. Grossmann and J. Morlet, “Decomposition of Hardy Functions into Square Integrable Wavelets of Constant Shape,” SIAM J. Math. Anal. Vol.15 no.4, July 1984.
2. M. Farge, “Wavelet Transforms and Their Applications to Turbulence,” Annu. Rev. Fluid Mech., vol.24, pp.395-457, 1992.
3. M. Farge, N. Kevlahan, V. Perrier, and E. Goirand, “Wavelts and Turbulence,” Proc. IEEE, vol.84, no.4, pp.639-669, April 1996.
4. B.Ph. van Milligen, E. Sanchez, T. Estrada, C. Hidalgo, and B. Branas, “Wavelet Bicoherence: A New Turbulence Analysis Tool,” Phys. Plasmas vol.2, no.8, pp.1-35, Aug. 1995. 3017.
5. V. Tarasov, E. Dubinin, S. Perraut, A. Roux, K. Sauer, A. Skalsky, and M. Delva, “Wavelet Application to the Magnetic Field Turbulence in the Upstream Region of the Martian Bow Shock,” Earth Planets Space, vol.50, p.699-708, 1998.
6. G. Buresti, G. Lombardi, and J. Bellazzini, “On the Analysis of Fluctuating Velocity Signals through Methods Based on the Wavelet and Hilbert Transforms,” Chaos Solitons & Fractals, vol.20, pp.149-158, 2004.
7. R. Carmona, W. L. Hwang, and B. Torresani, *Practical Time-Frequency Analysis*, Academic Press, 1998.
8. P. S. Addison, “Wavelet Analysis of the Breakdown of a Pulsed Vortex Flow,” Proc. Instn Mech. Engrs., vol.213 part C, pp.217-229, 1999.
9. Z. Zhang, H. Kwwabata, and Z. Q. Liu, “EEG Analysis Using Fast Wavelet Transform,” Proc. IEEE pp.2959, 2000.
10. S. J. Wu, “Instantaneous Properties of Low-Frequency Modulations and Three-Dimensionality Associated with Vortex Shedding,” Ph. D. Dissertation, National Cheng Kung University, June 2003.
11. J. J. Miau, S. J. Wu, C. C. Hu, and J. H. Chou, “Low Frequency Modulations Associated with Vortex Shedding form Flow over Bluff Body,” AIAA J., vol.42, no.7, pp.1388-1397, 2004.
12. S. J. Wu, J. J. Miau, C. C. Hu, and J. H. Chou, “On Low-Frequency Modulations an Three-Dimensionality in Vortex Shedding behind Flat Plates,” J. Fluid Mechanics, vol.526, pp.117-146, 2005.
13. J. K. Tu, J. J. Miau, J. H. Chou, and G. B. Lee, “Sensing Flow Separation on a Circular Cylinder

by MEMS Thermal-Film Sensors," AIAA paper No.2005-0299, 2005.

14. Y. N. Jeng, C. T. Chen, and Y. C. Cheng, "A New and Effective Tool to Look into Details of a Turbulent Data String," 12th National Computational Fluid Dynamics Conference, paper no. CFD 12-2501, Aug. 2005.
15. Y. N. Jeng and Y. C. Cheng, "A simple Strategy to Evaluate the Frequency Spectrum of a Time Series Data with Non-Uniform Intervals," Trans. Aero. Astro. Soc. R. O. C., vol.36, no.3, pp.207-214, 2004.
16. T. Irino and R. D. Patterson, "A Time-Domain, Level-Dependent auditory Filter: The Gammachirp". J.Acoust. Soc., Am. Vol.101, no.1, pp.412-419, Jan, 1997.
17. T. F. Quatieri, *Discrete-Time Speech Signal Processing, Principles and Practice*, Prince Hall Inc., 2002, chapter 11, pp.543-545.

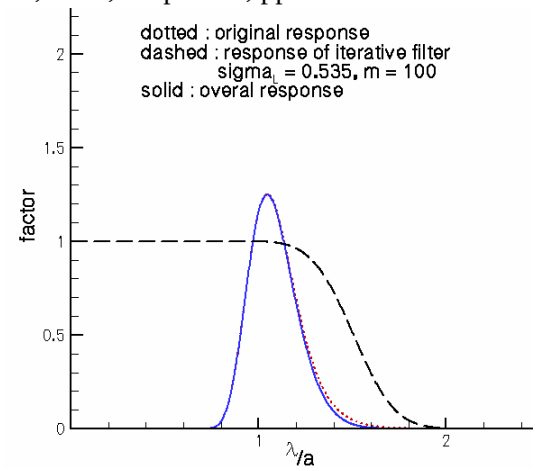

Fig.1 Responses of a single sine wave, $\sin(8\pi t),\ 0 \le t \le 20$, at $t = 9.0625$: dotted line is the original Morlet transform, dashed line is the single iterative filter with $\sigma = 0.535, m = 100$, and solid line is overall response fo the Morlet transform plus the filter.

(2a) (2b)

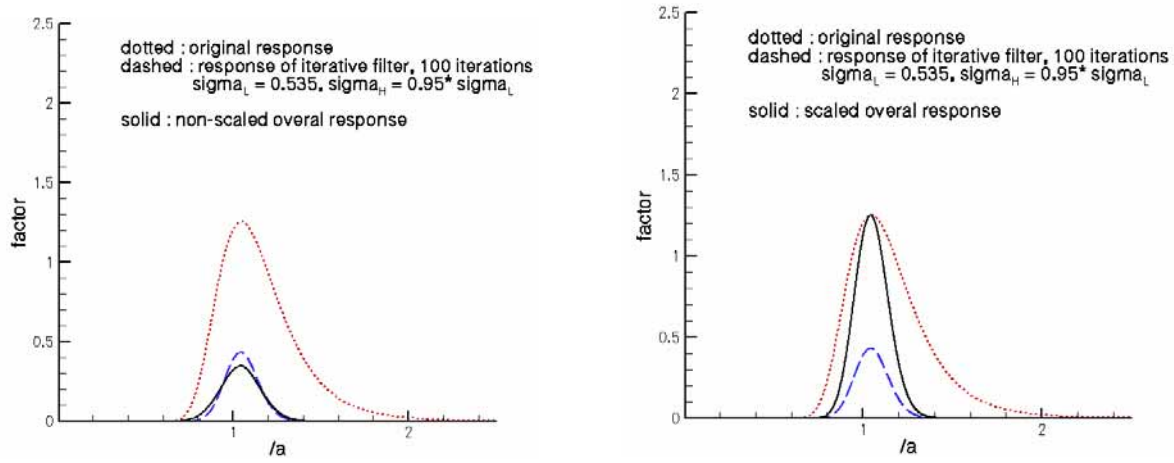

Fig.2 Responses of a single sine wave, $\sin(8\pi t),\ 0 \le t \le 20$, at $t = 9.0625$, the dotted line is the original Morlet transform, dashed line is the two-steps iterative filter with $\sigma_L = 0.535, \sigma_H = 0.95\sigma_L, m = 100$, and solid line is overall response of the Morlet transform plus the filter: (a) non-scaled overall response; and (b) scaled overall response.

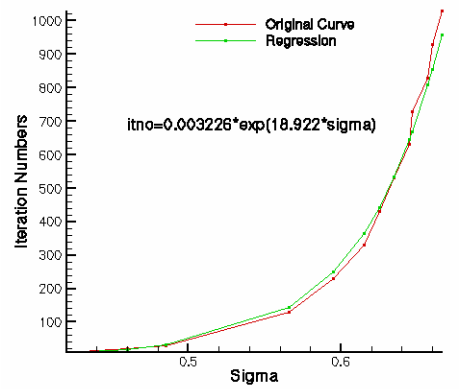

Fig.3 The necessary parameters of the iterative filter must be embedded into the Morlet transform so that the maximum factor is not changed.

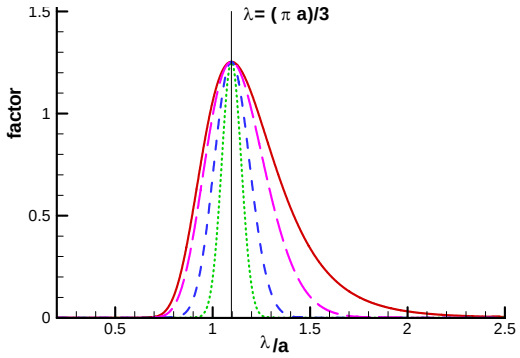

Fig.4 The responses of the original Morlet transform (solid line) and the enhanced transform embedded with the iterative filter with different parameters: long dashed line is the result of using $\sigma = 0.535, m = 100$, dashed line is that of $\sigma = 0.605, m = 400$, and the dotted line is that of $\sigma = 0.650, m = 1000$,

(5a)

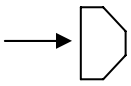

(5b)

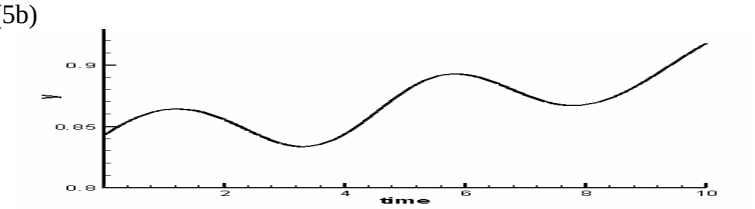

Fig.5 The removed smoothed and non-periodic part of the original data strings at : (5a) schematic diagram and (5b) $x = 5d$, respectively.

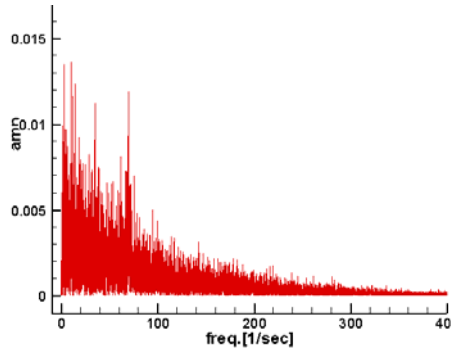

Fig.6 The spectrum corresponding to Fig.5.

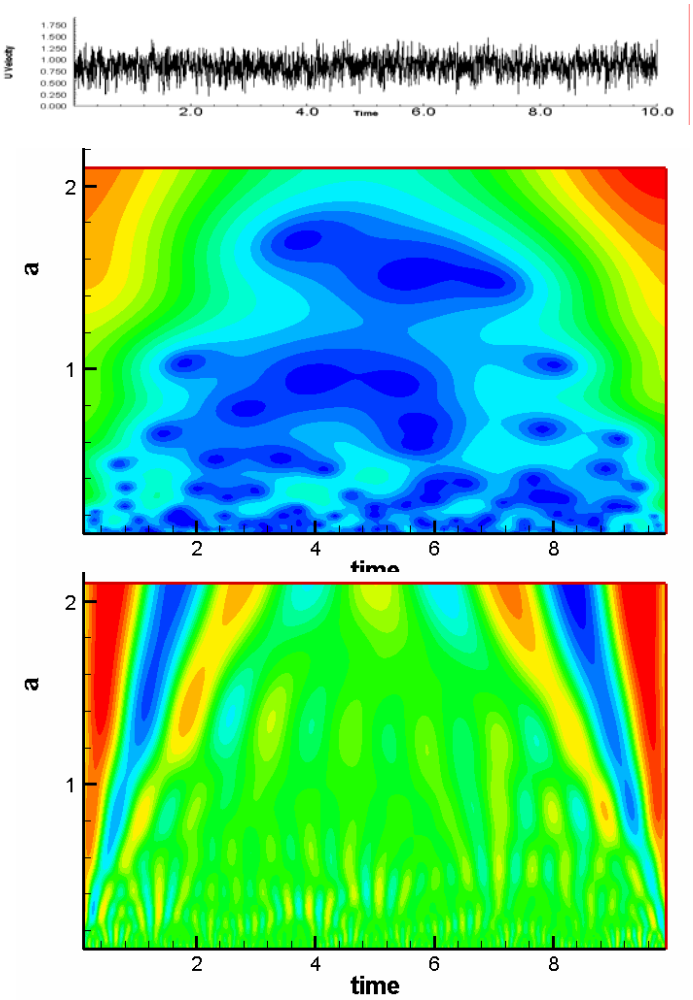

Fig.7 The results of employing the original Morlet transform, (a) top: the data without smoothed part; (b) the amplitude plot; and (c) the real part plot.

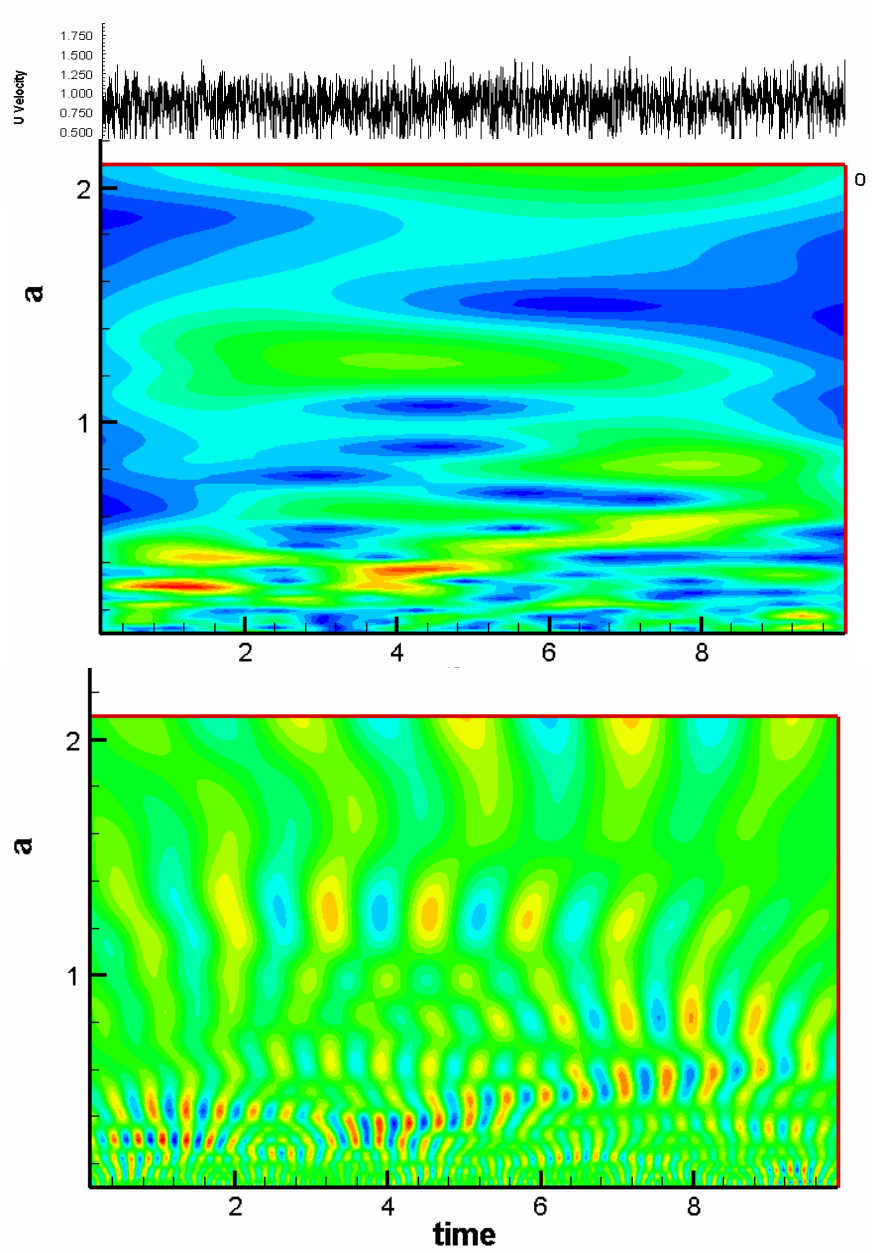

Fig.8 The results of employing the enhanced Morlet transform, (a) top: the data without smoothed part; (b) the amplitude plot; and (c) the real part plot.